ACS APPLIED MATERIALS & INTERFACES

Research Article

www.acsami.org

Colorimetric Sensing of Cu(II) in Aqueous Media with a Spiropyran Derivative via a Oxidative Dehydrogenation Mechanism

Yasuhiro Shiraishi,* Kazuya Tanaka, and Takayuki Hirai

Research Center for Solar Energy Chemistry and Division of Chemical Engineering, Graduate School of Engineering Science, Osaka University, Toyonaka 560-8531, Japan

Supporting Information

ABSTRACT: A spiropyran derivative containing a simple NO bidentate ligand (**2**) was synthesized. The ligand acts as a colorimetric chemodosimeter for selective Cu^{2+} detection in aqueous media. The ligand, even when treated at elevated temperature (60 °C), exists as a spirocyclic form and shows almost no absorption in the visible region. This is because the electron donation by an amine substituent suppresses spirocycle-opening. Treatment of the solution with Cu^{2+} at 60 °C, however, creates a strong absorption at 450−650 nm, whereas other metal cations do not promote spectral change. IR, NMR, and ab initio calculation revealed that Cu^{2+} is coordinated with two **2** ligands and produces 1:2 Cu^{2+}−amine complex intermediately. This is converted to the 1:2 Cu^{+}−imine complex via oxidative dehydrogenation of amine moieties, along with the reduction of Cu^{2+}. The formation of the imine complex decreases the electron density of nitrogen atoms and weakens the electron donation ability. This thus promotes thermal spirocycle opening and facilitates coloration of the solution.

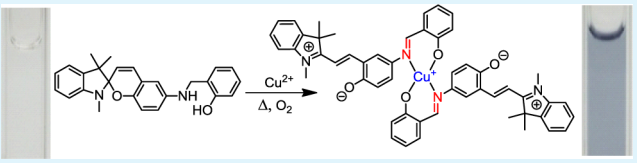

KEYWORDS: *colorimetric sensing, chemodosimeter, spiropyran, copper(II), isomerization*

1. INTRODUCTION

Cu^{2+} plays many important roles in biological processes such as gene expression, structural enhancement of proteins, and metalloenzymatic reactions.[1] Excess intake of Cu^{2+}, however, causes several neurodegenerative diseases such as Alzheimer disease,[2] amyotrophic lateral sclerosis,[3] Menkes and Wilson disease,[4] and prion disease.[5] Design of molecular receptors for selective and quantitative determination of Cu^{2+} has therefore attracted much attention because these receptors enable rapid determination of Cu^{2+} by simple spectroanalysis. A variety of fluorometric or colorimetric Cu^{2+} receptors have been proposed so far;[6−10] however, many show poor binding selectivity to Cu^{2+} over other cations such as Fe^{3+} and Hg^{2+} and lack sufficient selectivity.

Recently, reaction-based Cu^{2+} receptors called chemodosimeters have attracted much attention,[11−25] as an alternative to the classical chelation-based receptors. In most cases, colorless or nonemissive chemodosimeter molecules are converted to the colored or emissive molecules via Cu^{2+}-promoted irreversible chemical reactions. A variety of chemodosimeters for Cu^{2+} have been proposed based on several Cu^{2+}-promoted reactions such as hydrolysis[11−20] and oxidation.[21−25] Many of these chemodosimeters, however, suffer from several problems: (i) they act only in pure organic solvents or solutions with very small amounts of water (<20%);[13,19,22−24] (ii) they require specific reaction conditions such as acidic[16] or basic pH media;[11] and (iii) they show low Cu^{2+} selectivity in the presence of other metal cations.[15,17,19,25]

Earlier, we proposed a new Cu^{2+}-selective chemodosimeter, a boradiazaindacene (BODIPY) dye with an NO bidentate ligand (**1**), which facilitates fluorometric detection of Cu^{2+} via oxidative dehydrogenation of amine moiety (Scheme 1).[26] The ligand dissolved in aqueous media (pH 5−10) is nonfluorescent. Addition of Cu^{2+} to the solution leads to a formation of 1:2 Cu^{2+}−amine complex intermediately. This is transformed to the fluorescent 1:2 Cu^{+}−imine complex via oxidative dehydrogenation of amine moieties by Cu^{2+} and

Scheme 1. Proposed Mechanism for Cu^{2+}-Promoted Fluorescence Enhancement of the Chemodosimeter (1)[26]

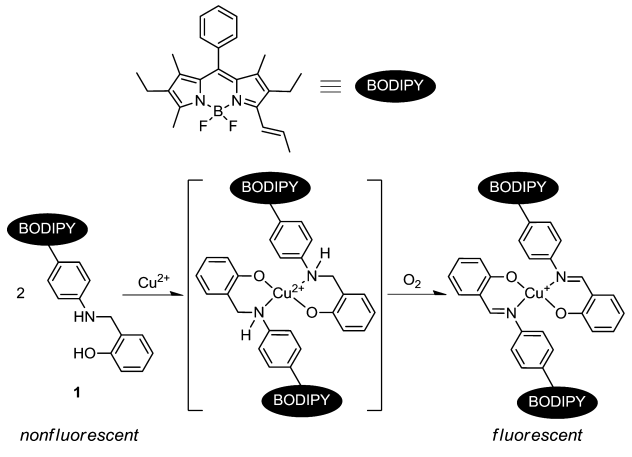

Received: February 14, 2013
Accepted: March 19, 2013
Published: March 19, 2013

   dx.doi.org/10.1021/am4005804 | ACS Appl. Mater. Interfaces 2013, 5, 3456−3463

molecular oxygen (O_2). The fluorescence response is selective to Cu^{2+} and is scarcely affected by other metal cations. The NO bidentate ligand therefore has a potential to enable design of Cu^{2+}-selective chemodosimeters.

Among the chemodosimeters, colorimetric ones are more advantageous than fluorometric ones due to the simplicity of sensing. The purpose of the present work is the design of colorimetric chemodosimeter for Cu^{2+} with the NO bidentate ligand. Spiropyran derivatives are a class of dyes that show reversible isomerization between the colorless spirocyclic (SP) form and colored spirocycle-opened merocyanine (MC) form upon heat or light stimulus (Scheme 2). The efficiency of SP → MC isomerization strongly depends on the strength of the spiro C−O bond of the SP form.[27] Substitution of electron-donating amino or methoxy group on the phenolate moiety (X) strengthens the spiro C−O bond and suppresses SP → MC isomerization.[28] In contrast, substitution of electron-withdrawing nitro or carbonyl group weakens the C−O bond and accelerates isomerization.[29]

Scheme 2. Isomerization of Spiropyran Derivatives between the SP and MC Forms upon Heat or Light Stimulus

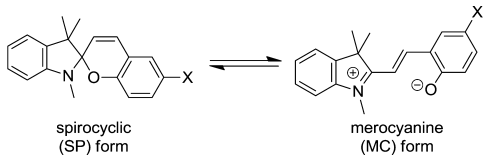

In the present work, we synthesized a spiropyran-based receptor containing NO bidentate ligand (**2**, Scheme 3) on the basis of the above SP → MC isomerization properties affected by substituents. We found that the ligand **2** acts as a chemodosimeter for colorimetric sensing of Cu^{2+} in aqueous media. The ligand dissolved in aqueous media exists as a SP form and shows almost no absorption in the visible region due to the electron donation by the amine substituent. Addition of Cu^{2+}, however, creates a strong absorption at 450−650 nm. This colorimetric response is due to the formation of 1:2 Cu^{+}−imine complex by the dehydrogenation of amine moieties, as is the case for compound **1**.[26] The formation of this complex suppresses the electron donation from the nitrogen atoms and weakens the spiro C−O bond. This thus promotes SP → MC isomerization and results in coloration of the solution.

Scheme 3. Synthesis of the Chemodosimeter 2

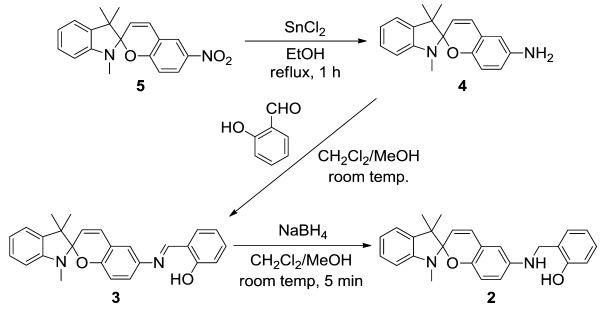

2. RESULTS AND DISCUSSION

2.1. Synthesis and Isomerization Properties of Compounds. The ligand **2** was synthesized by three steps as shown in Scheme 3. A nitro-substituted spiropyran (**5**) was reduced with $SnCl_2$, affording amine derivative (**4**) with 63% yield. Condensation of **4** with *o*-salicylaldehyde gave imine derivative (**3**) with 51% yield. This was then reduced with $NaBH_4$, affording **2** with 54% yield. These intermediates and products were fully characterized by NMR and MS analysis (Figures S1−S11, Supporting Information).

Isomerization properties of compounds **2** and **3** were studied first. Figure 1 shows the time-dependent change in absorption spectra of **2** and **3** (20 μM) measured in a buffered water/MeCN mixture (1/1 v/v; pH 7.0) at 60 °C in the dark condition. Almost no absorption in the visible region indicates that these compounds exist in solution as SP form, and thermal SP → MC isomerization does not occur. As shown by blue line in Figure 2, thermal SP → MC isomerization proceeds on the ground-state potential surface and involves two step reactions such as (i) spiro C−O bond cleavage ($^0E_{cleavage}$) and (ii) cis → trans isomerization ($^0E_{rotation}$).[30] Both **2** and **3** have high energy for C−O bond cleavage ($^0E_{cleavage}$) because electron-donating amine and imine substituents strengthen the C−O bond. This suppresses the C−O bond cleavage and, hence, does not promote thermal SP → MC isomerization.

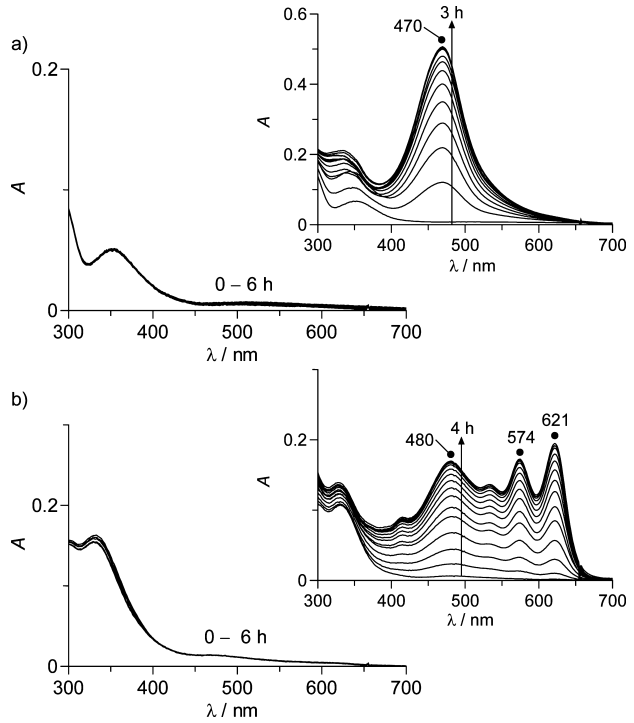

Figure 1. Time-dependent change in the absorption spectra of (a) **2** and (b) **3** (20 μM) in a buffered water/MeCN mixture (1/1 v/v; HEPES 100 mM, pH 7.0) measured at 60 °C in the dark condition. (inset) Change in absorption spectra measured at 25 °C under UV irradiation (254 nm).

The inset of Figure 1a shows the change in absorption spectra of **2** measured at 25 °C under UV irradiation (254 nm). **2** exhibits an absorption band at 470 nm assigned to the MC form. This is confirmed by ab initio calculation performed on the Gaussian 03 program[31] based on the time-dependent density functional theory (TDDFT).[32] Table 1 summarizes the calculated excitation energies for respective transitions of the MC form of **2**. Singlet excitation of **2**(MC) is mainly contributed by highest occupied molecular orbital (HOMO) → low unoccupied molecular orbital (LUMO) (S_0 → S_1)

dx.doi.org/10.1021/am4005804 | ACS Appl. Mater. Interfaces 2013, 5, 3456−3463

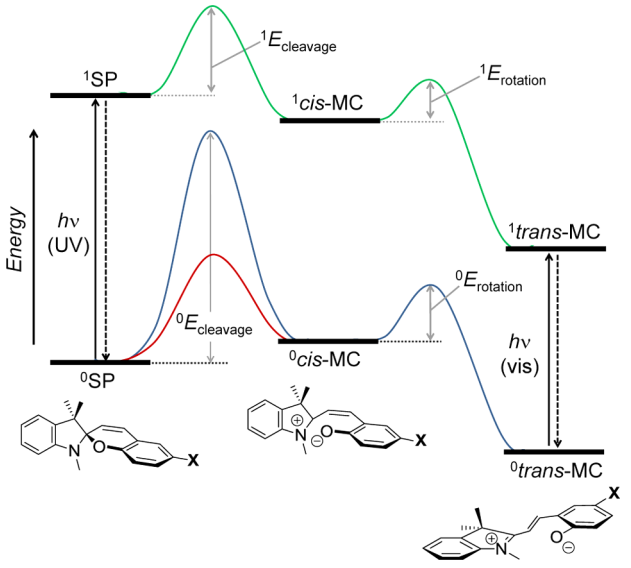

Figure 2. Potential energy surface for ring-opening/closing reactions of spiropyran derivatives.

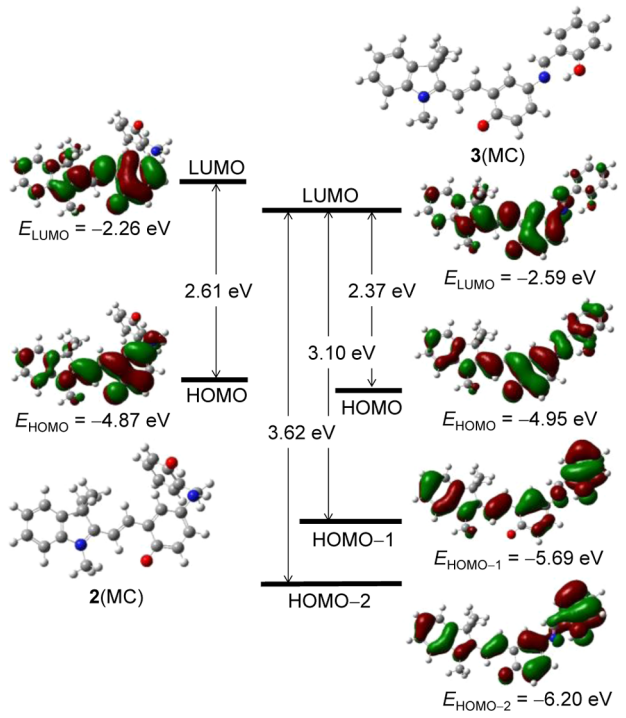

Figure 3. Energy diagrams for main orbitals of **2**(MC) and **3**(MC), calculated at the DFT level (B3LYP/6-31G).

transition. Its energy (2.51 eV, 493 nm) is close to the observed absorption maxima (470 nm), and total change in dipole moment is determined to be 5.85 D. As shown in Figure 3 (left), electrons of HOMO and LUMO are distributed over the indole and phenolate moieties, indicating that the 470 nm absorption is assigned to the intramolecular charge transfer from phenolate to indole moiety.[33]

As shown in the inset of Figure 1b, UV irradiation of **3** exhibits three absorption bands assigned to the MC form at 480, 574, and 621 nm, respectively. As shown in Table 1, electronic excitation of **3**(MC) is contributed by HOMO → LUMO ($S_0 \rightarrow S_1$), HOMO − 1 → LUMO ($S_0 \rightarrow S_2$), and HOMO − 2 → LUMO ($S_0 \rightarrow S_3$) transitions. Their respective energies are 2.07 (600), 2.23 (555), and 2.54 eV (487 nm) and are close to the observed absorption maxima (621, 574, and 480 nm). As shown in Figure 3 (right), electrons of LUMO, HOMO, HOMO − 1, and HOMO − 2 are distributed over the molecules. As shown in Table 1, total changes in dipole moment for the respective transitions are determined to be 10.8, 11.1, and 17.2 D. These indicate that three absorption bands for **3**(MC) are due to the intramolecular charge transfer from the phenolate to indole moiety.

The SP → MC isomerization of **2** and **3** promoted by UV irradiation is because it occurs on the excited state potential surface. As shown by the green line in Figure 2, photoisomerization involves two step reactions such as spiro C−O bond cleavage ($^1E_{cleavage}$) and cis → trans isomerization ($^1E_{rotation}$), similar to thermal isomerization (blue line). The activation energies in the excited state are lower than those in the ground state.[30] This thus promotes SP → MC photoisomerization of **2** and **3.** These suggest that **2** and **3** do not undergo thermal SP → MC isomerization due to the electron-donating amine and imine substituents.

2.2. Colorimetric Sensing of Cu^{2+}. Figure 4a shows the absorption spectra of **2** (20 μM) measured in a water/MeCN mixture (1/1 v/v; pH 7.0) with or without each respective metal cation (2 equiv) at 60 °C in the dark condition. **2** shows almost no absorption of the MC form. Addition of Cu^{2+}, however, creates a strong absorption at 450−650 nm. In contrast, other metal cations do not show spectral change (Figure 4b). This suggests that Cu^{2+} selectively promotes spectral change of **2**. It is noted that the spectral change is unaffected by other metal cations (Figure S12, Supporting Information), as is the case for compound **1**.[26] This suggests that **2** selectively detects Cu^{2+} even in the presence of other metal cations.

As shown in Figure 5, the Cu^{2+}-induced spectral change of **2** occurs at broad pH range (5−11). In addition, Cu^{2+} salts with different counteranions such as $Cu(CH_3COO)_2$, $CuCl_2$,

Table 1. Electronic Excitation Properties of 2(MC) and 3(MC) Determined by TDDFT Calculations

species		CIC[a]	E/eV [λ/nm]	μ/Debye				f
				μ_x	μ_y	μ_z	μ_{total}	
2(MC)	$S_0 \rightarrow S_1$	HOMO → LUMO (0.605)	2.5134 [493.29]	−5.26	−2.55	−0.239	5.85	0.7015
	$S_0 \rightarrow S_2$	HOMO − 3 → LUMO (0.685)	2.7084 [457.78]	−3.49	0.824	0.844	3.68	0.0001
	$S_0 \rightarrow S_3$	HOMO − 1 → LUMO (0.703)	2.9269 [423.60]	16.5	−16.7	1.61	23.5	0.0183
3(MC)	$S_0 \rightarrow S_1$	HOMO → LUMO (0.612)	2.0667 [599.93]	5.22	−9.43	−0.776	10.8	0.3428
	$S_0 \rightarrow S_2$	HOMO − 1 → LUMO (0.583)	2.2345 [554.86]	−4.57	−11.1	−0.702	11.1	0.2037
	$S_0 \rightarrow S_3$	HOMO − 2 → LUMO (0.485)	2.5448 [487.20]	19.5	−11.4	−0.711	17.2	0.1975

[a]CI expansion coefficients for the main orbital transitions.

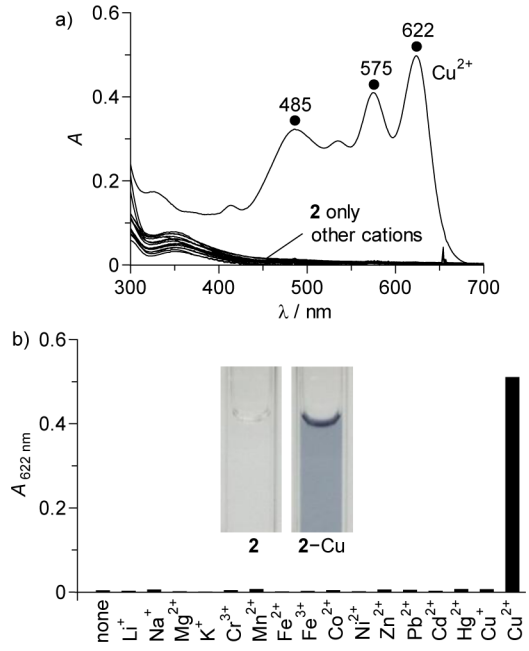

Figure 4. (a) Absorption spectra of **2** (20 μM) measured in a buffered water/MeCN mixture (1/1 v/v; HEPES 100 mM, pH 7.0) with each respective metal cation (2 equiv). (b) Absorbance of solutions at 622 nm. The respective spectra were measured after stirring the solution for 6 h at 60 °C.

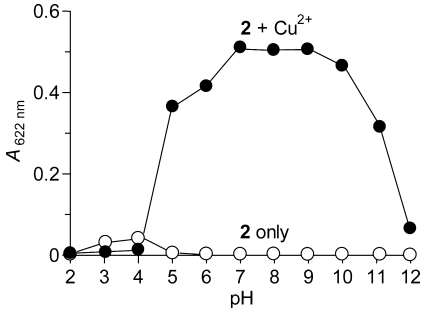

Figure 5. Absorbance at 622 nm of a water/MeCN mixture (1/1 v/v) containing **2** (20 μM) at different pH, measured with or without Cu^{2+} (2 equiv). Each spectrum was measured after stirring the solution for 6 h at 60 °C.

$Cu(ClO_4)_2$, and $Cu(NO_3)_2$ show similar spectral change (Figure S13, Supporting Information). Figure 6 shows the results of absorption titration of **2** with Cu^{2+}. Stepwise addition

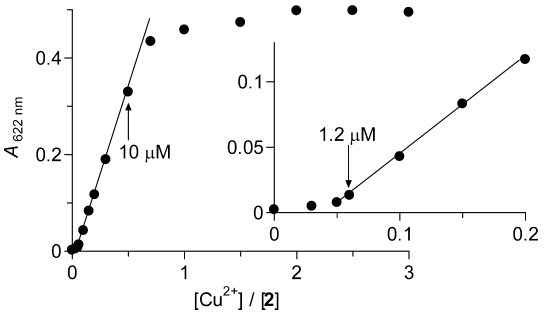

Figure 6. Absorption titration of **2** (20 μM) with Cu^{2+} performed in a buffered water/MeCN mixture (1/1 v/v; pH 7.0). Each data was obtained after stirring the solution at 60 °C for 6 h.

of Cu^{2+} leads to an increase in the absorption band. A liner relationship in the range of 1.2–10 μM Cu^{2+} indicates that **2** enables accurate determination of Cu^{2+} in this concentration range. The detection limit, 1.2 μM, is below the maximum permissive level of Cu^{2+} in drinking water (~20 μM) set by the US Environmental Protection Agency (EPA),[34] suggesting that **2** enables sensitive Cu^{2+} detection.

2.3. Determination of Colored Species. An excess amount of EDTA, when added to the colored solution obtained after treatment of **2** with Cu^{2+}, does not show any spectral change (Figure S14, Supporting Information). This indicates that **2** reacts with Cu^{2+} irreversibly, as does compound **1**.[26] As shown in Figure 7, Job's plot shows a maximum absorption at X (= $[Cu^{2+}]/([Cu^{2+}] + [\mathbf{2}])$) = 0.33. These data clearly suggest that irreversible 1:2 reaction of Cu^{2+} with **2** produces colored species.

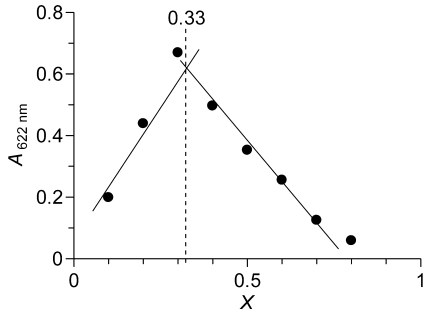

Figure 7. Job's plot of **2** with Cu^{2+} (X = $[Cu^{2+}]/([Cu^{2+}] + [\mathbf{2}])$). The total concentration of **2** and Cu^{2+} is set at 40 μM.

As shown in Scheme 4, 1:2 reaction of Cu^{2+} with **2** occurs via three steps and finally produces the 1:2 Cu^{+}–imine complex with MC moieties, resulting in coloration of the solution. IR analysis confirms the involvement of imine moiety in the colored species. The colored solution was extracted with CH_2Cl_2, washed with water, and concentrated by evaporation. Figure 8 shows the IR spectra of **2** and the obtained 1:2 complex. **2** shows a band assigned to N–H stretching vibration for amine group at 3423 cm^{-1}. In contrast, the 1:2 complex does not show this band but shows a new band at 1620 cm^{-1} assigned to imine moiety, which is observed for the reference compound, **3**, which also contains an imine moiety. In addition, the absorption spectrum of the MC form of **3** produced by UV irradiation (Figure 1b) is very similar to that of the 1:2 complex (Figure 4). These findings indicate that the colored 1:2 complex involves both MC and imine moieties.

As shown in Figure S15 (Supporting Information), ESR analysis of the 1:2 complex shows no Cu^{2+} signal, indicating that the complex does not involve Cu^{2+}. As reported,[35] Cu^{3+} is easily reduced to Cu^{2+} by $K_4[Fe(CN)_6]$. Addition of an excess amount of $K_4[Fe(CN)_6]$ to the solution containing the 1:2 complex does not show any spectral change (Figure S16, Supporting Information), indicating that Cu^{3+} is also not involved. These indicate that Cu^{+} is involved in the complex, as is the case for compound **1**.[26] As shown in Figure S17 (Supporting Information), MALDI-TOF MS analysis of a colored solution shows a peak at m/z 932.5, which is assigned to a [1:2 Cu^{+}–imine MC complex + $2Na^{+}$ + $2OH^{-}$] ion. These data suggest that, as shown in Scheme 4, the coloration of solution is due to the formation of the 1:2 Cu^{+}–imine MC complex.

dx.doi.org/10.1021/am4005804 | ACS Appl. Mater. Interfaces 2013, 5, 3456–3463

Scheme 4. Proposed Mechanism for Cu^{2+}-Selective Ring-Opening of Spiropyran Moieties of 2 at 60 °C

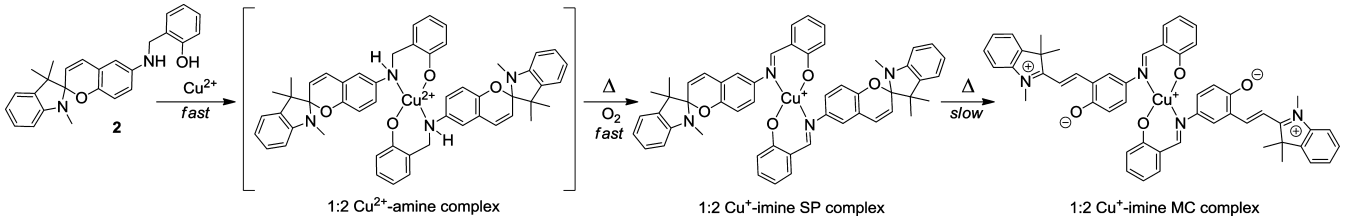

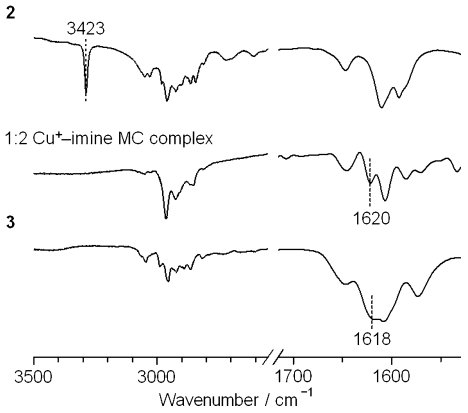

Figure 8. IR spectra of **2**, **3**, and 1:2 Cu^{+}–imine MC complex.

2.4. Reaction Sequence. As shown in Scheme 4, 2 reacts with Cu^{2+} via three steps: (i) coordination of Cu^{2+} with two **2** ligands produces the 1:2 Cu^{2+}–amine complex intermediately; (ii) conversion to the 1:2 Cu^{+}–imine complex containing SP moiety via oxidative dehydrogenation of the amine unit; and, (iii) thermal SP → MC isomerization and production of the 1:2 Cu^{+}–imine MC complex. This sequence is confirmed by ^{1}H NMR and absorption spectra. As shown in Figure 9a, **2** shows $-NH-CH_2-$ protons (H^b and H^c) at 5.5 and 4.1 ppm. As shown in Figure 9b, the solution, when stirred with Cu^{2+} for 3 min at 60 °C, leads to a disappearance of these protons and creates a new singlet signal (H^a) assigned to imine proton at 8.9 ppm. This indicates that Cu^{2+} immediately coordinates with **2** and produces the 1:2 Cu^{+}–imine complex. In this spectrum, two singlet signals for magnetically nonequivalent methyl protons still appear at 1.1–1.2 ppm, and *N*-methyl proton remains unchanged at ca. 2.6 ppm, indicating that an SP moiety is involved in the complex. These signals are very similar to those for compound **3** with an imine moiety (Figure 9d). This indicates that reaction of **2** with Cu^{2+} rapidly produces the 1:2 Cu^{+}–imine SP complex. The rapid formation of the complex is confirmed by the time-dependent change in absorption spectra. As shown in Figure 10a, addition of Cu^{2+} to the solution containing **2** immediately creates an absorption band at 356 nm within 3 min, assigned to the ligand-to-metal charge transfer (LMCT) band from Schiff base ligand to metal cation.[36] It must be noted that the 1:2 Cu^{+}–imine SP complex does not form under argon atmosphere. This suggests that, as shown in Scheme 4, the complex is produced via oxidative dehydrogenation of two amine moieties by Cu^{2+} and O_2, as is the case for compound **1**.[26]

The 1:2 Cu^{+}–imine SP complex then undergoes thermal SP → MC isomerization. As shown in Figure 9c, the solution containing the 1:2 Cu^{+}–imine SP complex, when stirred for 6 h at 60 °C, leads to disappearance of two singlet signals for nonequivalent methyl protons at 1.1–1.2 ppm, along with an appearance of one singlet signal at 1.2 ppm. This indicates that the methyl protons of SP form become magnetically equivalent due to the isomerization to planar MC form.[37] In addition, the *N*-methyl proton shifts downfield from 2.6 to 3.5 ppm due to the quaternarization of indole nitrogen.[38] These data clearly support the formation of the 1:2 Cu^{+}–imine MC complex. As shown in Figure 10a, the increase in MC absorption band is associated with a decrease in LMCT band for the 1:2 Cu^{+}–

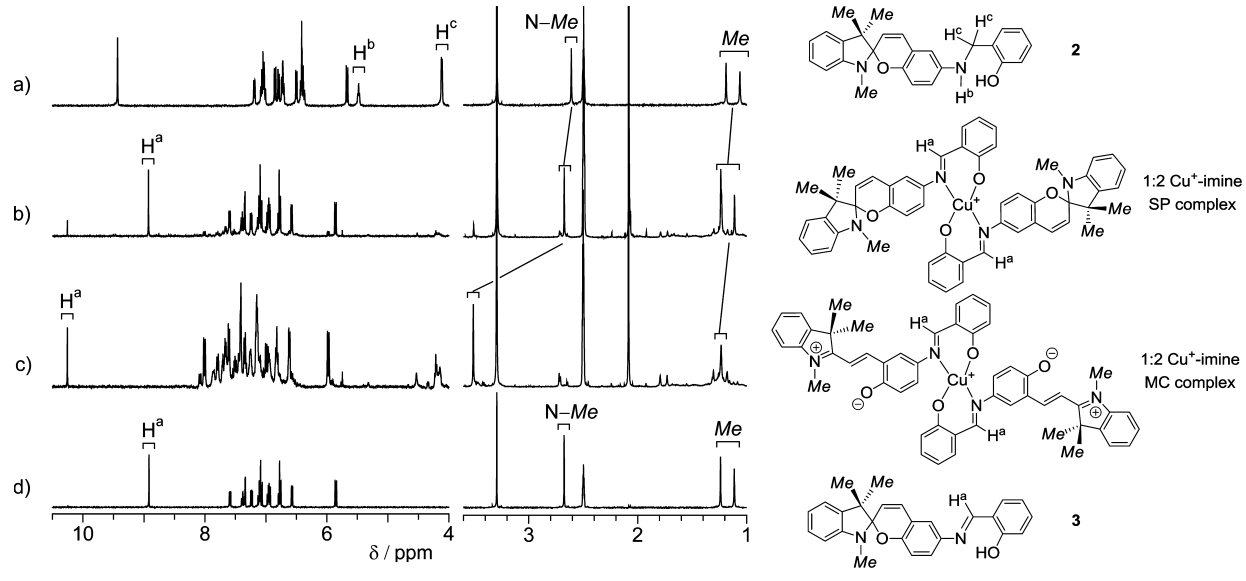

Figure 9. ^{1}H NMR spectra (DMSO-d_6, 400 MHz) of (a) **2**, (b) 1:2 Cu^{+}–imine SP complex, (c) 1:2 Cu^{+}–imine MC complex, and (d) **3**.

dx.doi.org/10.1021/am4005804 | ACS Appl. Mater. Interfaces 2013, 5, 3456–3463

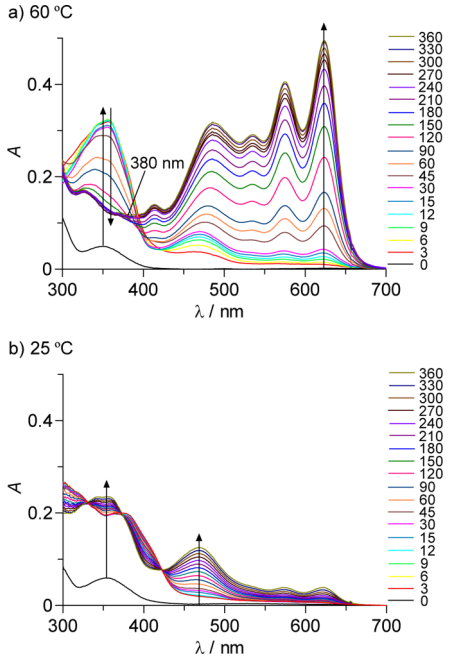

Figure 10. Time-dependent change in absorption spectra of **2** (20 μM) in a buffered water/MeCN mixture (1/1 v/v; HEPES 100 mM, pH 7.0) measured with Cu^{2+} (4 equiv) at different temperature. The numbers on the right side denote the time for reaction (min).

imine SP complex at 356 nm. These NMR and absorption data clearly support the reaction sequence in Scheme 4.

The 1:2 Cu^{+}–imine SP complex promotes thermal SP → MC isomerization, but compounds **2** and **3** do not (Figure 1). This is because the formation of imine complex decreases the electron-donating ability of a nitrogen atom adjacent to spiropyran moiety. This is confirmed by Mulliken atomic charge on the nitrogen atom determined by ab initio calculation. As shown in Figure 11, Mulliken charges on the nitrogen atoms of **2** and **3** are −0.732 and −0.601, respectively. In contrast, the charge on the 1:2 Cu^{+}–imine SP complex is more positive (−0.547), suggesting that the electron-donating ability of the 1:2 Cu^{+}–imine SP complex is indeed much lower than that of **2** and **3**. This is due to the LMCT from the imine nitrogen to Cu^{+}.[36] This thus weakens the spiro C–O bond and deceases the activation energy for its cleavage ($^{0}E_{cleavage}$), as depicted by the red line in Figure 2. This therefore promotes thermal SP → MC isomerization of the 1:2 Cu^{+}–imine SP complex.

2.5. Effects of Temperature and Visible Light Irradiation. As summarized in Scheme 4, the reaction of **2** with Cu^{2+} at 60 °C produces the 1:2 Cu^{+}–imine SP complex very rapidly (within 3 min), and subsequent SP → MC isomerization is the rate-determining step for coloration. This reaction sequence depends strongly on temperature. As shown in Figure 10b, the solution containing **2** and Cu^{2+}, when treated at 25 °C, shows an increase in the LMCT band at 356 nm occurring much more slowly than that treated at 60 °C. This means that oxidative dehydrogenation of the 1:2 Cu^{2+}–amine complex by Cu^{2+} and O_2 occurs very slowly at lower temperature. In addition, as shown in Figure 12, the increase in MC absorption band is much slower at lower temperature. These data suggest that both imine complex formation and SP → MC isomerization occur slowly at lower temperature and relatively high temperature is necessary for Cu^{2+} sensing.

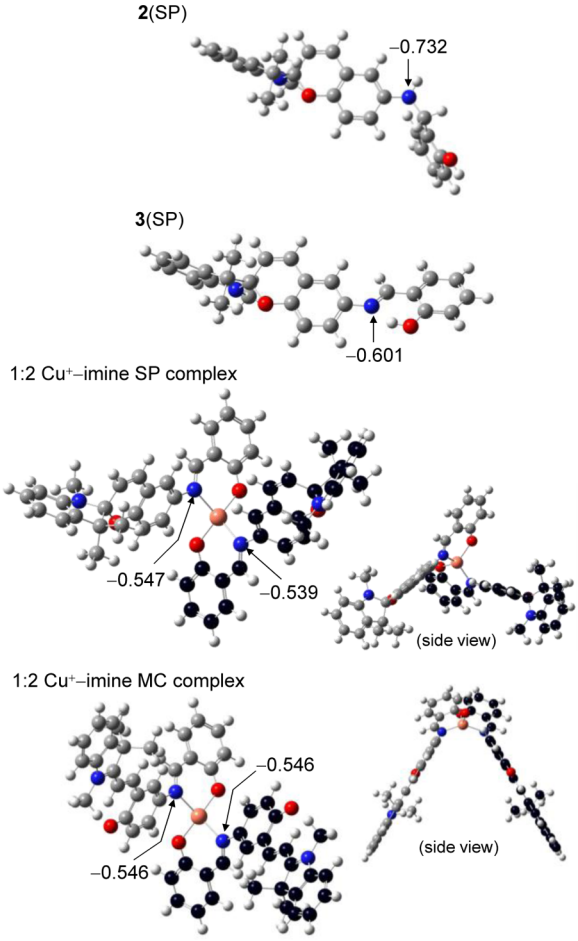

Figure 11. Geometry optimized structures and Mulliken charges of the nitrogen atoms for **2**(SP), **3**(SP), 1:2 Cu^{+}–imine SP complex, and 1:2 Cu^{+}–imine MC complex (B3LYP/6-31G/LANL2DZ). The gray (black), blue, red, orange, and white atoms denote C, N, O, Cu, and H atoms, respectively.

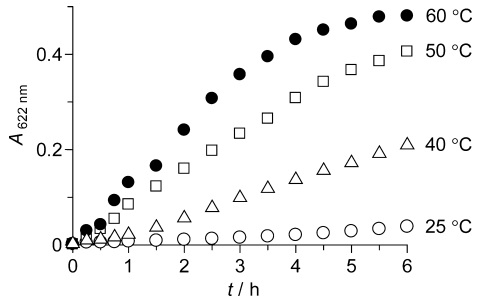

Figure 12. Time-dependent changes in the absorbance at 622 nm of **2** (20 μM) measured in a buffered water/MeCN mixture (1/1 v/v; HEPES 100 mM, pH 7.0) with Cu^{2+} (4 equiv) at different temperature.

It is well-known that the MC form undergoes reversion to the SP form under visible light irradiation.[27] The 1:2 Cu^{+}–imine MC complex, however, does not revert to the SP form. As shown in Figure S18 (Supporting Information), the absorption spectrum of the 1:2 Cu^{+}–imine MC complex scarcely changes even by visible light irradiation at 470 nm. Similar behaviors are observed for the MC forms of **2** and **3**. As shown by the green line in Figure 2, photochemical MC → SP reversion occurs on the excited state potential surface via the

dx.doi.org/10.1021/am4005804 | ACS Appl. Mater. Interfaces 2013, 5, 3456–3463

photoexcitation of the MC form and involves trans → cis isomerization and C−O recombination. As reported,[39] the MC form is highly stabilized in aqueous media by H-bonding interaction, and their ground and excited states lie on significantly lower levels than the corresponding SP form. This therefore results in higher activation energy of trans → cis isomerization and suppresses MC → SP reversion.

CONCLUSION

We found that a spiropyran derivative with simple NO bidentate ligand (**2**) acts as a colorimetric chemodosimeter for selective Cu^{2+} detection in aqueous media when treated at 60 °C. The ligand exists as a SP form and shows almost no absorption in the visible region, because the electron donation by amine substituent suppresses thermal isomerization to MC form. In contrast, the treatment with Cu^{2+} shows a strong absorption in the visible region. This colorimetric response is due to the formation of a 1:2 Cu^{+}−imine MC complex, which is produced by sequential reactions: (i) coordination of Cu^{2+} with **2** (formation of the 1:2 Cu^{2+}−amine complex), (ii) oxidative dehydrogenation of amine moieties by Cu^{2+} and O_2 (formation of the 1:2 Cu^{+}−imine SP complex), and (iii) thermal SP → MC isomerization of the complex (formation of the 1:2 Cu^{+}−imine MC complex). The formation of the 1:2 Cu^{+}−imine SP complex decreases the electron-donating ability of nitrogen atoms and promotes SP → MC isomerization. The coloration response is selective to Cu^{2+}, and other metal cations do not affect the response. Although the Cu^{2+} sensing requires relatively high temperature (60 °C) and long time (6 h), the molecular design presented here, which controls the electron-donating ability of substituent by the coordination of targeted metal cations leading to spirocycle opening, may contribute to the design of a more efficient and useful chemodosimeter for colorimetric sensing of trace amount of metal cations.

EXPERIMENTAL METHODS

Materials. All of the reagents used were supplied by Wako, Aldrich, and Tokyo Kasei and used as received. Perchlorate salts (Li^{+}, Na^{+}, Mg^{2+}, K^{+}, Cr^{3+}, Mn^{2+}, Fe^{2+}, Fe^{3+}, Co^{2+}, Ni^{2+}, Zn^{2+}, Pb^{2+}, Cd^{2+}, Hg^{2+}, and Cu^{2+}) and iodide salt (Cu^{+}) were used as the metal cation source. Water was purified by the Milli-Q system.

Synthesis of 4. **5**[40] (964 mg, 3.0 mmol) and $SnCl_2{\cdot}2H_2O$ (3.4 g, 15 mmol) were refluxed in EtOH (20 mL) for 1 h under N_2. The resulting $SnCl_2$ was removed by filtration, and the solution was concentrated by evaporation. NaOH (5%, 50 mL) was added to the residue, and the organic phase was extracted with $CHCl_3$ (25 mL × 2). The organic layer was washed with water, dried over Na_2SO_4, and concentrated by evaporation. The resultant was purified by silica gel column chromatography with ethyl acetate, affording **4** as a brown solid (560 mg, 63%). ^{1}H NMR ($CDCl_3$, 400 MHz, TMS): δ (ppm) = 7.15 (t, 1H, J = 7.33 Hz), 7.06 (d, 1H, J =7.33 Hz), 6.81 (t, 1H, J = 7.33 Hz), 6.74 (d, 1H, J = 10.08 Hz), 6.42−6.55 (m, 4H), 5.66 (d, 1H, J = 10.08 Hz), 3.34 (s, 2H), 2.71 (s, 3H), 1.29 (s, 3H), 1.15 (s, 3H). ^{13}C NMR ($CDCl_3$, 101 MHz): δ (ppm) =148.3, 147.7, 139.2, 137.0, 129.2, 127.5, 121.5, 120.2, 119.2, 118.9, 117.0, 115.5, 113.3, 106.7, 103.6, 51.5, 28.9, 25.9, 20.3. MS (EI): calcd for $C_{19}H_{20}N_2O$ 292.4 found m/z 292.2. HRMS (EI) m/z calcd for $C_{19}H_{20}N_2O$ 292.1576 found 292.1547.

Synthesis of 3. **4** (202 mg, 0.68 mmol) and *o*-salicylaldehyde (570 μL, 5.4 mmol) were stirred in a mixture of CH_2Cl_2 (51 mL) and MeOH (34 mL) at room temperature until the complete disappearance of **4** by TLC monitoring. The solution was concentrated by evaporation and was purified by silica gel column chromatography with ethyl acetate/*n*-hexane (2/1 v/v), affording **3** as a yellow solid (140 mg, 51%). ^{1}H NMR (DMSO-d_6, 400 MHz, TMS): δ (ppm) = 13.21 (s, 1H), 8.92 (s,1H), 7.59 (d, 1H, J = 6.10 Hz), 7.38 (t, 1H, J = 6.95 Hz), 7.35 (d, 1H, J = 2.68 Hz), 7.22−7.25 (m, 1H), 7.06−7.13 (m, 3H), 6.93−6.98 (m, 2H), 6.76−6.80 (m, 2H), 6.57 (d, 1H, J = 7.81 Hz), 5.86 (d, 1H, J = 10.25 Hz), 2.68 (s, 3H), 1.24 (s, 3H), 1.11 (s, 3H). ^{13}C NMR ($CDCl_3$, 101 MHz): δ (ppm) =161.0, 160.2, 153.9, 148.1, 140.8, 136.7, 132.7, 131.9, 129.0, 127.7, 122.2, 121.5, 120.5, 119.6, 119.4, 119.3, 119.3, 119.0, 117.2, 115.8, 106.9, 104.7, 51.9, 28.9, 25.9, 20.2. MS (FAB): calcd for $C_{26}H_{24}N_2O_2$ 396.5 found m/z 396.6. HRMS (EI) m/z calcd for $C_{26}H_{24}N_2O_2$ 396.1838 found 396.1858.

Synthesis of 2. **3** (110 mg, 0.28 mmol) was dissolved in a mixture of CH_2Cl_2 (26 mL) and MeOH (18 mL). $NaBH_4$ (21.6 mg, 0.56 mmol) was added to the solution and stirred for 5 min. The resultant was concentrated by evaporation and brine was added to the residue. The solution was extracted with CH_2Cl_2, and the obtained organic layer was dried over Na_2SO_4 and concentrated by evaporation. The resultant was purified by silica gel column chromatography with ethyl acetate/*n*-hexane (1/2 v/v), affording **2** as a white solid (59.2 mg, 54%). ^{1}H NMR (DMSO-d_6, 400 MHz, TMS): δ (ppm) = 9.43 (s, 1H), 7.19 (d, 1H), 7.01−7.09 (m, 3H), 6.85 (d, 1H, J = 10.25 Hz), 6.79 (d, 1H, J = 8.05 Hz), 6.71−6.74 (m, 2H), 6.50 (d, 1H, J = 7.80 Hz), 6.37−6.44 (m, 3H), 5.67 (d, 1H, J = 10.25 Hz), 5.48 (t, 1H, J = 5.86 Hz), 4.12 (d, 2H, J = 5.86 Hz), 2.61 (s, 3H), 1.19 (s, 3H), 1.06 (s, 3H). ^{13}C NMR ($CDCl_3$, 101 MHz): δ (ppm) = 157.2, 149.5, 148.2, 139.9, 136.8, 129.2, 129.2, 128.5, 127.6, 122.8, 121.5, 120.4, 119.9, 119.2, 119.1, 118.4, 116.7, 115.6, 114.7, 106.8, 104.0, 51.7, 50.3, 28.9, 25.9, 20.2. MS (FAB): calcd for $C_{26}H_{26}N_2O_2$ 398.5 found m/z 398.3. HRMS (EI) m/z calcd for $C_{26}H_{26}N_2O_2$ 398.1994 found 398.2014.

Computational Methods. Preliminary geometry optimizations were performed using the WinMOPAC version 3.0 software (Fujitsu Inc.) at the semiempirical PM3 level.[41,42] The obtained structures were fully refined with tight convergence criteria at the DFT level with the Gaussian 03 package, using the B3LYP function. Metal-free compounds were calculated using the 6-31G basis set. Cu^{+} complexes were calculated using the 6-31G basis set for all atoms except for Cu, for which LANL2DZ basis set with effective core potential was used. The excitation energies and oscillator strengths of each structure were calculated by TD-DFT at the same level of optimization using the polarizable continuum model (PCM)[43] with water as a solvent.

Analysis. Absorption spectra were measured on a UV−visible spectrophotometer (Shimadzu, Multispec-1500) using a 10-mm path length quartz cell under aerated condition. UV or visible light irradiation was carried out with a Xe lamp (300 W; Asahi Spectra Co. Ltd.; Max-302) equipped with 254 or 470 nm band-pass filter (LX334 and LX470; light intensity, 1.10 W m^{-2}).[44,45] ^{1}H and ^{13}C NMR spectra were obtained by a JEOL JNM-AL400 and JEOL JNM-GSX270 Excalibur using TMS as standard. EI and FAB-MS spectra were obtained on JEOL JMS 700 spectrometer. MALDI-TOF MS chart was obtained with Shimadzu/Kratos AXIMA-CFR spectrometer.[46] IR spectra were measured on an FTIR-610 infrared spectrophotometer (Jasco Corp.) with KBr disk. ESR spectra were performed at X-band using a Bruker EMX-10/12 spectrometer with a 100 kHz magnetic field modulation at a microwave power level of 20 mW.[47]

ASSOCIATED CONTENT

Supporting Information

Characterization data for compounds (Figures S1−S11), effect of other metal cations on absorption increase (S12), effect of Cu^{2+} salts (S13), effect of EDTA (S14), ESR spectra for Cu complex (S15), effect of $K_4[Fe(CN)_6]$ (S16), MALDI−TOF MS charts of Cu (S17), effect of visible light irradiation (S18), and Cartesian coordinates for compounds. This material (PDF) is available free of charge via the Internet at http://pubs.acs.org.

AUTHOR INFORMATION

Corresponding Author

*E-mail: shiraish@cheng.es.osaka-u.ac.jp.

Notes

The authors declare no competing financial interest.

■ ACKNOWLEDGMENTS

This work was supported by the Grant-in-Aid for Scientific Research (No. 21760619) from the Ministry of Education, Culture, Sports, Science and Technology, Japan (MEXT). We thank Prof. Yoshito Tobe and Dr. Kazukuni Tahara (Osaka University) for MALDI-TOF MS analysis.

■ REFERENCES

(1) Linder, M. C.; Hazegh−Azam, M. *Am. J. Clin. Nutr.* **1996**, *63*, 797S−811S.
(2) Barnham, K. J.; Masters, C. L.; Bush, A. I. *Nat. Rev. Drug Discov.* **2004**, *3*, 205−214.
(3) Valentine, J. S.; Hart, P. J. *Proc. Natl. Acad. Sci.* **2003**, *100*, 3617−3622.
(4) Waggoner, D. J.; Bartnikas, T. B.; Gitlin, J. D. *Neurobiol. Dis.* **1999**, *6*, 221−230.
(5) Brown, D. R.; Kozlowski, H. *Dalton Trans.* **2004**, 1907−1917.
(6) Suresh, M.; Ghosh, A.; Das, A. *Chem. Commun.* **2008**, 3906−3908.
(7) Royzen, M.; Dai, Z.; Canary, J. W. *J. Am. Chem. Soc.* **2005**, *127*, 1612−1613.
(8) Wang, S.; Men, G.; Zhao, L.; Hou, Q.; Jiang, S. *Sensor. Actuators B* **2010**, *145*, 826−831.
(9) Jiang, J.; Jiang, H.; Tang, X.; Yang, L.; Dou, W.; Liu, W.; Fang, R.; Liu, W. *Dalton Trans.* **2011**, *40*, 6367−6370.
(10) Yang, Y.; Huo, F.; Yin, C.; Chu, Y.; Chao, J.; Zhang, Y.; Zhang, J.; Li, S.; Lv, H.; Zheng, A.; Liu, D. *Sensor. Actuators B* **2013**, *177*, 1189−1197.
(11) Li, N.; Xiang, Y.; Tong, A. *Chem. Commun.* **2010**, *46*, 3363−3365.
(12) Kovács, J.; Mokhir, A. *Inorg. Chem.* **2008**, *47*, 1880−1882.
(13) Kovács, J.; Rödler, T.; Mokhir, A. *Angew. Chem., Int. Ed.* **2006**, *45*, 7815−7817.
(14) Qi, X.; Jun, E. J.; Xu, L.; Kim, S. −J.; Hong, J. S. J.; Yoon, Y. J.; Yoon, J. *J. Org. Chem.* **2006**, *71*, 2881−2884.
(15) Mokhir, A.; Krämer, R. *Chem. Commun.* **2005**, 2244−2246.
(16) Kim, M. H.; Jang, H. H.; Yi, S.; Chang, S. −K.; Han, M. S. *Chem. Commun.* **2009**, 4838−4840.
(17) Yu, M.; Shi, M.; Chen, Z.; Li, F.; Li, X.; Gao, Y.; Xu, J.; Yang, H.; Zhou, Z.; Yi, T.; Huang, C. *Chem.—Eur. J.* **2008**, *14*, 6892−6900.
(18) Dujols, V.; Ford, F.; Czarnik, A. W. *J. Am. Chem. Soc.* **1997**, *119*, 7386−7387.
(19) Yu, M. −M.; Li, Z. −X.; Wei, L. −H.; Wei, D. −H.; Tang, M. −S. *Org. Lett.* **2008**, *10*, 5115−5118.
(20) Huo, F. −J.; Yin, C. −X.; Yang, Y. −T.; Su, J.; Chao, J. −B.; Liu, D. −S. *Anal. Chem.* **2012**, *84*, 2219−2223.
(21) Lin, W.; Long, L.; Chen, B.; Tan, W.; Gao, W. *Chem. Commun.* **2010**, *46*, 1311−1313.
(22) Ajayakumar, G.; Sreenath, K.; Gopidas, K. R. *Dalton Trans.* **2009**, 1180−1186.
(23) Kennedy, D. P.; Kormos, C. M.; Burdette, S. C. *J. Am. Chem. Soc.* **2009**, *131*, 8578−8586.
(24) Senthilvelan, A.; Ho, I. −T.; Chang, K. −C.; Lee, G. −H.; Liu, Y. −H.; Chung, W. −S. *Chem.—Eur. J.* **2009**, *15*, 6152−6160.
(25) Liu, J.; Lu, Y. *J. Am. Chem. Soc.* **2007**, *129*, 9838−9839.
(26) Wang, D.; Shiraishi, Y.; Hirai, T. *Chem. Commun.* **2011**, *47*, 2673−2675.
(27) Minkin, V. I. *Chem. Rev.* **2004**, *104*, 2751−2776.
(28) Zaichenko, N. L.; Lyubimov, A. V.; Marevtsev, V. S.; Cherkashin, M. I. *Bull. Acad. Sci. USSR, Div. Chem. Sci.* **1987**, *7*, 1543−1544.
(29) Zaichenko, N. L.; Kol'tsova, L. S.; Shiyonok, A. I.; Venidiktova, O. V.; Barachevsky, V. A.; Marevtsev, V. S. *Russ. Chem. Bull. Int. Ed.* **2005**, *54*, 2612−2615.
(30) Sheng, Y.; Leszczynski, J.; Garcia, A. A.; Rosario, R.; Gust, D.; Springer, J. *J. Phys. Chem. B* **2004**, *108*, 16233−16243.
(31) Frisch, M. J.; Trucks, G. W.; Schlegel, H. B.; Scuseria, G. E.; Robb, M. A.; Cheeseman, Jr. J. R.; Montgomery, J. A.; Vreven, T.; Kudin, K. N.; Burant, J. C.; Millam, J. M.; Iyengar, S. S.; Tomasi, J.; Barone, V.; Mennucci, B.; Cossi, M.; Scalmani, G.; Rega, N.; Petersson, G. A.; Nakatsuji, H.; Hada, M.; Ehara, M.; Toyota, K.; Fukuda, R.; Hasegawa, J.; Ishida, M.; Nakajima, T.; Honda, Y.; Kitao, O.; Nakai, H.; Klene, M.; Li, X.; Knox, J. E.; Hratchian, H. P.; Cross, J. B.; Bakken, V.; Adamo, C.; Jaramillo, J.; Gomperts, R.; Stratmann, R. E.; Yazyev, O.; Austin, A. J.; Cammi, R.; Pomelli, C.; Ochterski, J. W.; Ayala, P. Y.; Morokuma, K.; Voth, G. A.; Salvador, P.; Dannenberg, J. J.; Zakrzewski, V. G.; Dapprich, S.; Daniels, A. D.; Strain, M. C.; Farkas, O.; Malick, D. K.; Rabuck, A. D.; Raghavachari, K.; Foresman, J. B.: Ortiz, J. V.; Cui, Q.; Baboul, A. G.; Clifford, S.; Cioslowski, J.; Stefanov, B. B.; Liu, G.; Liashenko, A.; Piskorz, P.; Komaromi, I.; Martin, R. L.; Fox, D. J.; Keith, T.; Al-Laham, M. A.; Peng, C. Y.; Nanayakkara, A.; Challacombe, M.; Gill, P. M. W.; Johnson, B.; Chen, W.; Wong, M. W.; Gonzalez, C.; Pople, J. A. *Gaussian 03*, Revision B.05; Gaussian, Inc., Wallingford CT, 2004.
(32) Stratmann, R. E.; Scuseria, G. E.; Frisch, M. J. *J. Chem. Phys.* **1998**, *109*, 8218−8224.
(33) Hasegawa, J.; Bureekaew, S.; Nakatsuji, H. *J. Photochem. Photobiol. A: Chem.* **2007**, *189*, 205−210.
(34) Xu, X.; Daniel, W. L.; Wei, W.; Mirkin, C. A. *Small* **2010**, *6*, 623−626.
(35) Margerum, D. W.; Chellappa, K. L.; Bossu, F. P.; Burce, G. L. *J. Am. Chem. Soc.* **1975**, *97*, 6894−6896.
(36) Medzhidov, A. A.; Fatullaeva, P. A.; Peng, S. M.; Ismaiylov, R. G.; Lee, G. H.; Garaeva, S. R. *Russ. J. Coord. Chem.* **2012**, *38*, 126−133.
(37) Natali, M.; Aakeröy, C.; Desper, J.; Giordani, S. *Dalton Trans.* **2010**, *39*, 8269−8277.
(38) Yagi, S.; Nakamura, S.; Watanabe, D.; Nakazumi, H. *Dyes Pigm.* **2009**, *80*, 98−105.
(39) Shiraishi, Y.; Itoh, M.; Hirai, T. *Phys. Chem. Chem. Phys.* **2010**, *12*, 13737−13745.
(40) Raymo, F. M.; Giordani, S. *J. Am. Chem. Soc.* **2001**, *123*, 4651−4652.
(41) Shiraishi, Y.; Saito, N.; Hirai, T. *J. Am. Chem. Soc.* **2005**, *127*, 8304−8306.
(42) Shiraishi, Y.; Saito, N.; Hirai, T. *J. Am. Chem. Soc.* **2005**, *127*, 12820−12822.
(43) Cossi, M.; Barone, V.; Cammi, R.; Tomasi, J. *Chem. Phys. Lett.* **1996**, *255*, 327−335.
(44) Shiraishi, Y.; Sumiya, S.; Hirai, T. *Chem. Commun.* **2011**, *47*, 4953−4955.
(45) Shiraishi, Y.; Matsunaga, Y.; Hirai, T. *Chem. Commun.* **2012**, *48*, 5485−5487.
(46) Tobe, Y.; Umeda, R.; Iwasa, N.; Sonoda, M. *Chem.—Eur. J.* **2003**, *9*, 5549−5559.
(47) Tsukamoto, D.; Shiraishi, Y.; Sugano, Y.; Ichikawa, S.; Tanaka, S.; Hirai, T. *J. Am. Chem. Soc.* **2012**, *134*, 6309−6315.